Geophys. J. R. astr. Soc. (1973) **31**, 433–445.

A Magnetotelluric Traverse in Southern Australia

H. Y. Tammemagi and F. E. M. Lilley

(Received 1972 September 12)

Summary

Telluric potentials were recorded at nine sites stretching 1000 km from east of Wilcannia (N.S.W.) to west of Coober Pedy (S.A.) in south central Australia. These were combined with data obtained from a simultaneous magnetic variometer study, and analysed to yield magnetotelluric impedance tensors. The estimation of probable errors for the impedance tensors was an important part of the calculations. Numerical calculations for two-dimensional models showed that the observed data could be explained by a conductive-resistive-conductive layering. The top conductive (10 ohm-m) layer is approximately 5 km deep and the ensuing resistive section (1000 ohm-m) continues to a depth of about 230 km. This is underlain by an indeterminably thick conductive layer. Embedded in this general structure is an extremely good conductor (0·1 ohm-m) which strikes north–south. The detection of this good conductor is the main result of this work. The good conductor lies just east of the Adelaide Geosyncline at a depth of a few kilometres, and is of minimum thickness 10 km. It is thought to be related to the accretion of the eastern portion of the Australian continent on to the stable western Precambrian platform by tectonic processes. The strong anisotropy present in the magnetotelluric data at all sites could not be explained by induction in conductive sediments, and is thought to be caused by localized conductivity inhomogeneities distorting current flow.

Introduction

Since its introduction by Cagniard (1953) as a possible geophysical tool, the contributions of the magnetotelluric (M–T) method to the understanding of the Earth have been rather indefinite. An early compilation of M–T results by Fournier (1962) showed that not only are the data very scattered, but also the apparent resistivity curves obtained at any one site from orthogonal magnetic and electric components are invariably widely different; that is, anisotropic. Performing a telluric traverse in conjunction with a magnetometer array study in southern Australia provided an excellent opportunity to examine some of these inconsistencies. The Australian inland provides a laboratory generally free of any cultural electromagnetic noise, and there is little topographic variation to perturb the telluric currents. Most important, however, is the opportunity which arises of comparing the electrical conductivity structure derived from the magnetotelluric data with the results obtained independently from the magnetometer array study.

This paper presents the results of the magnetotelluric analysis only. A separate paper is in preparation by Gough, McElhinny & Lilley (1973), describing the magnetometer array experiment in detail; it has already been mentioned briefly by Gough, Lilley & McElhinny (1972).

Geology

The area under study lies across the Adelaide Geosyncline joining the two contrasting regions on either side. To the west lies Precambrian shield and to the east a succession of generally younger rocks; however the zone of demarcation is not clear and occasional Precambrian outcrops have been found to the east. The two regions differ in heat flow, the eastern region having a value generally higher than that of the west (Jaeger 1970). The travel times of seismic waves also show a difference, being greater to the east (Cleary, Simpson & Muirhead 1972). The Adelaide Geosyncline, marking the line of division, appears to be the southern extremity of a major crustal feature, the Fitzroy–Spencer fracture zone. Studies of Australian seismicity by Doyle, Everingham & Sutton (1968) and others have been interpreted in terms of plate tectonics by Cleary & Simpson (1971), who suggest that this fracture zone separates two adjacent crustal blocks. The geosyncline was formed by a great orogeny, in the late Cambrian to Ordovician, of vast accumulated sediments; at present, the area is one of complexity and fracturing, and is a major source of seismicity.

The experiment

The array of 25 magnetic variometers was in operation for approximately three months, from mid-September to early December 1970. By contrast, all telluric observations were made with just three recording units. These were set up at the three eastern-most stations of the line and run simultaneously for 1 month, then shifted westward to three new localities for the next month, and finally moved once more. A total of nine stations was thus occupied by the telluric instruments, and these are shown in Fig. 1 together with the sites of the array magnetometers. Table 1 lists the magnetotelluric sites, their code names, and their geographic coordinates, in addition to their dates of operation. The installation and operation of the telluric apparatus was independent of the magnetometer array maintenance.

Three identical telluric recording instruments were especially built for this investigation. Arucomp 4100 recorders (manufactured by Hartmann and Braun) were modified to operate from car batteries for continuous periods of about 10 days. The potential differences, between lead plates buried 500 m apart, were measured with an accuracy of better than 0·5 mv km^{-1}. Each instrument recorded two channels: the telluric potentials in the magnetic north and east directions, (designated A and B respectively). The potentials were filtered and recorded directly onto 10-day chart paper by ink ribbon, using a dotting interval of 10 s. Timing marks were recorded manually at the start and finish of the chart with the aid of a Bulova Accutron clock, synchronized to radio time signals. The instruments were successfully tested prior

Table 1

Yelta	Yel	31° 56′ S,	143° 39′ E	1970 Sept. 11–Oct. 6
Hazelvale	Haz	31° 46′ S,	142° 16½′ E	1970 Sept. 11–Oct. 6
Mulyungarie	Mly	31° 33′ S,	140° 47½′ E	1970 Sept. 9 –Oct. 7
Waukaringa (Melton)	Wak	32° 20′ S,	139° 21′ E	1970 Oct. 8 –Nov. 3
Partacoona	Par	32° 0½′ S,	138° 9½′ E	1970 Oct. 9 –Nov. 3
Pimba (Woomera)	Pim	31° 8′ S,	136° 48½′ E	1970 Oct. 10–Nov. 4
Billa Kalina	Bil	29° 55′ S,	136° 11½′ E	1970 Nov. 5 –Dec. 4
Ingomar	Ing	29° 38½′ S,	134° 48′ E	1970 Nov. 6 –Dec. 3
Tallaringa	Tal	28° 56½′ S,	133° 59½′ E	1970 Nov. 7 –Dec. 2

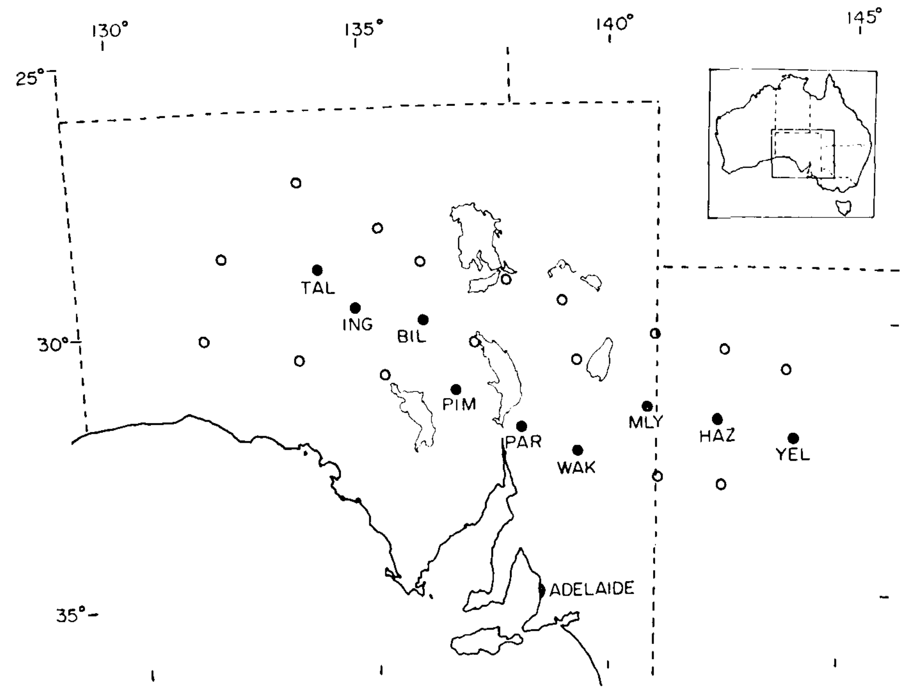

FIG. 1. The geographic location of the M–T traverse in southern Australia. Both telluric and magnetic data were obtained at the sites marked by solid circles, magnetic data only at open circles.

to this study and the results have been reported elsewhere (Lilley & Tammemagi 1972).

The magnetometers were of the type described by Gough & Reitzel (1967). The principle of operation is classical, with magnets suspended on torsion fibres deflecting light beams across photographic film. The three orthogonal magnetic elements, H, D, Z, were recorded at 10-s intervals to an accuracy of better than one gamma (nanoTesla). The instruments were battery powered and ran unattended for periods of three weeks. Hourly timing marks were recorded automatically as deflections in the traces by Bulova Accutron time pieces.

By recording electromagnetic phenomena in the period range of minutes to several hours, it was possible to obtain electrical conductivity information from a few kilometres to a few hundred kilometres depth.

The impedance tensor

The impedance tensor, Z_{ij}, is defined by

$$\left.\begin{aligned} E_1 &= Z_{11}H_1+Z_{12}H_2 \\ E_2 &= Z_{21}H_1+Z_{22}H_2 \end{aligned}\right\} \qquad (1)$$

where E_i and H_i denote components of the electric and magnetic field respectively (Cantwell 1960). Equation (1) is the mathematical statement that a particular component of the electric field can be induced linearly not only by the magnetic field orthogonal to it, but also by the parallel component. In the case of departure from a layered laterally homogeneous Earth, the impedance tensor is a very diagnostic set of parameters. For a two-dimensional Earth with the measuring axes aligned parallel and perpendicular to the axis of strike, the impedance tensor becomes

$$\left.\begin{aligned} Z_{11} &= Z_{22} = 0 \\ Z_{12} &\neq -Z_{21}\,. \end{aligned}\right\} \tag{2}$$

Thus, if a two-dimensional structure is present it should be possible to computationally rotate the impedance tensor, testing whether equation (2) is satisfied for any particular angle of rotation. Usually the diagonal elements Z_{11} and Z_{22} will have minima. These may, however, not be zero, and to determine whether a two-dimensional interpretation is reasonable a skew coefficient can be formed (Swift 1967)

$$\text{skew} = |Z_{11}+Z_{22}|/|Z_{12}-Z_{21}|\,.$$

The skew is invariant under rotation and approaches zero for a two-dimensional structure.

Analysis and results

The magnetic film records and the telluric charts were visually inspected, and seven sections were chosen for analysis. These are listed in Table 2 with times in G.M.T. Fig. 2 illustrates some of these events. The data were chosen so that each section contained one or more complete transient events, such as sub-storms or bays.

Enlarged Xerox charts were prepared from the chosen magnetic films and these, together with the telluric charts, were digitized at 30-s intervals. To avoid aliasing problems it was first necessary to smooth the high frequency events manually. The subsequent analyses were performed on an IBM 360/50 computer at the Australian National University Computer Centre.

A major feature of the data analysis method is to treat transient events which have been recorded in full. Then any one particular event is independent of those before and after it, and the earlier and later portions of the record may be put equal to zero. The spectrum obtained by Fourier transformation of such a time series is then, in principle, valid for all frequencies. If for example the event is a truncated sinusoidal variation, then the side lobes in the spectrum can be used for analysis as well as the main peak. If there are two such independent events the impedance tensor can be solved using equation (1). Denoting the event numbers by superscripts one obtains

$$Z_{xy} = \begin{vmatrix} H_x{}^1 & E_x{}^1 \\ H_x{}^2 & E_x{}^2 \end{vmatrix} \Bigg/ \begin{vmatrix} H_x{}^1 & H_y{}^1 \\ H_x{}^2 & H_y{}^2 \end{vmatrix} \tag{3}$$

and similar equations for the other tensor elements Z_{yx}, Z_{xx} and Z_{yy}. It is apparent from the denominator that the solution is indeterminate if the magnetic polarizations are not different for the two events.

One advantage of calculating the impedance tensors by this method is that errors can be assigned to the tensor elements in a straightforward manner. Defining a probable error as one which has a 50 per cent probability of being exceeded, it can

Table 2

Event No. 1	1970.	Oct. 4	09 : 30–15 : 30
2		Sept. 13	03 : 00–17 : 00
3		Sept. 14	10 : 30–16 : 30
4		Oct. 16	09 : 00–22 : 00
5		Oct. 23	12 : 30–18 : 00
6		Nov. 7	00 : 00–16 : 00
7		Nov. 15–16	23 : 00–02 : 00

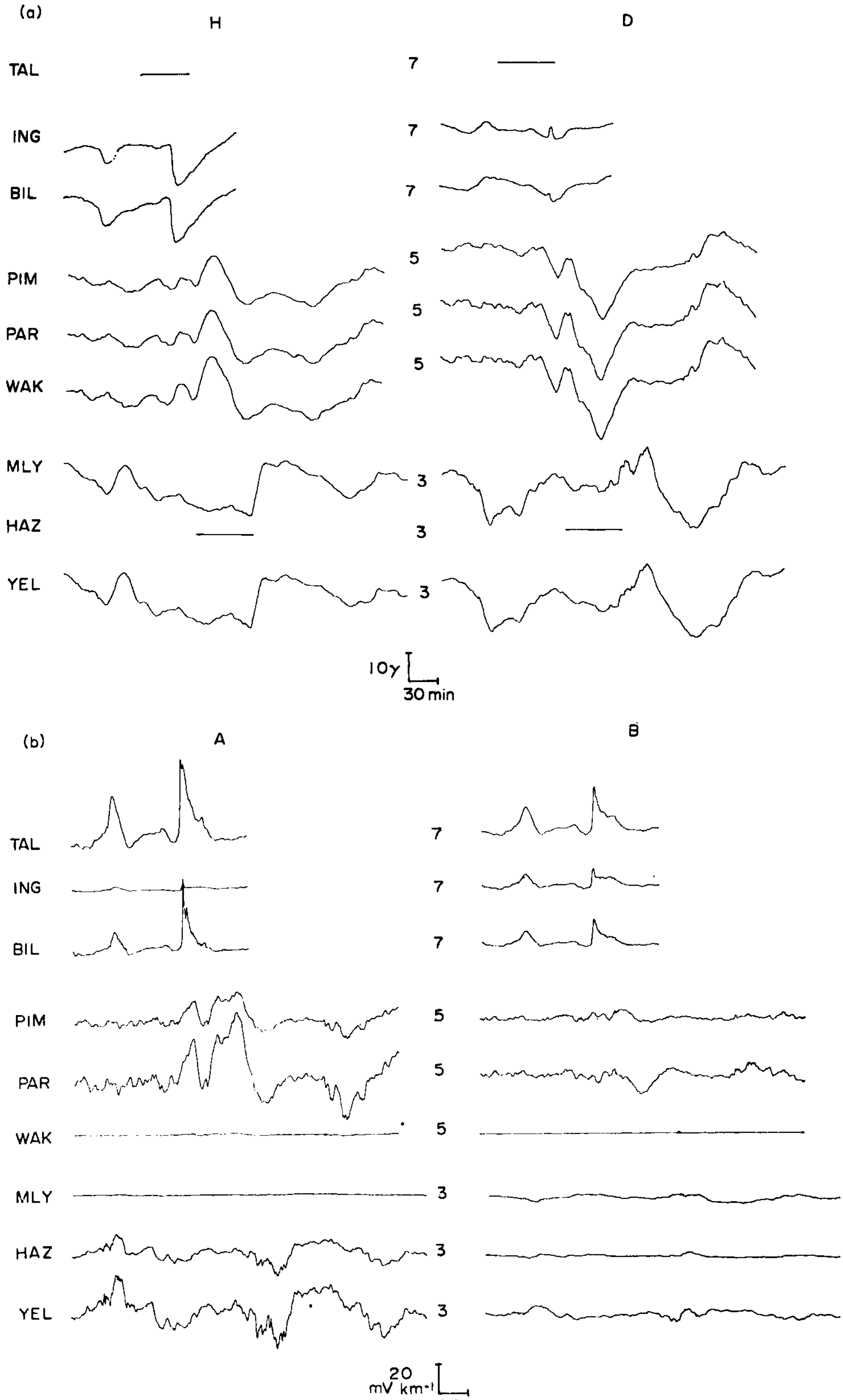

FIG. 2. Simultaneous telluric and magnetic recordings in three stages across the array. (H—magnetic north, D—magnetic east, A—telluric north, B—telluric east). The figures in the centre represent event numbers (see Table 2).

be shown that the probable error of a Fourier coefficient is $(2/n)^{\frac{1}{2}}q$, (Whittaker & Robinson 1946, p. 280), where n is the number of data points and q is the probable error in each. It is then straightforward to carry errors through the calculations of equation (3). It is important to note that equation (3) is composed entirely of complex quantities and therefore there are a large number of operations involved in computing the impedance tensor. Hence the probable error accrues rapidly.

Having carried out the error calculations thus far, a further refinement is available in the determination of the tensor value. If several isolated events are considered, say three, pairs can be formed in three ways. For each pair a solution for Z is available via equation (3) with a probable error. In this case there are three solutions with attendant probable errors and from them a weighted average can be formed (Bevington 1969, p. 70).

The sections of data in Table 2 were subdivided into separate transient events. Each datum point in the original time series was assigned a probable error of one gamma or 1 mv km^{-1}, as an estimate of accumulated errors such as those due to instrument drift, calibration and chart digitization. Linear trends were removed to ensure that no effects of longer period phenomena like the diurnal variation were involved, and then impedance tensors and their probable errors were calculated by the method just described. Fig. 3 shows the results for Yelta, and it is seen that at long periods the impedance tensors are stable and have reasonable errors. However, as the periods decrease the fluctuations of the tensor elements increase as do their errors; in fact, at a period of about 500 s the probable errors become larger than the values to which they refer. It was decided that a fractional probable error of greater than one was too large to be acceptable, and all such values were subsequently disregarded. This discrimination had the effect of imposing a serious high frequency cut-off to the data.

In order to widen the frequency band-width, the original data were searched again for transient events of high frequency content. Trains of micropulsations, characteristically of period 1–3 mins, were found in bursts throughout the records. These proved to be ideal; the ones chosen were digitized manually and analysed by the method described above.

To obtain further statistical smoothing of the results, the impedance tensor element values were band-width averaged.

Skew coefficients were calculated, and as an example those for Yelta are shown in Fig. 4. There are no strict rules for the interpretation of skew coefficients, but values

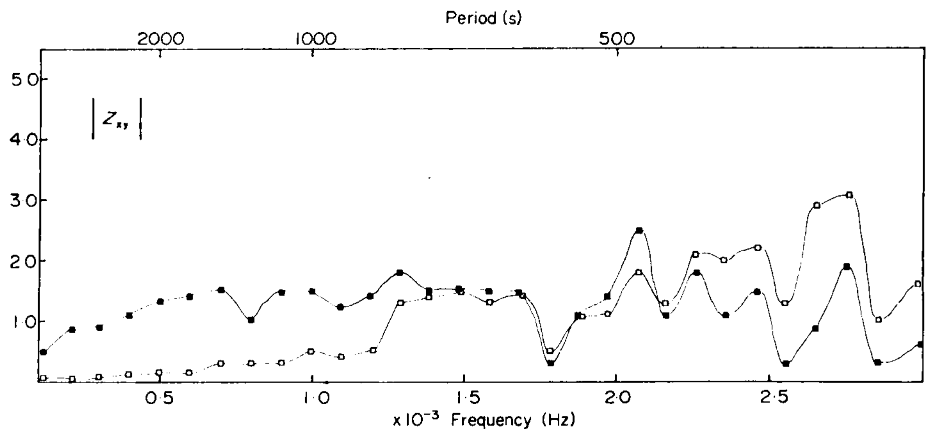

FIG. 3. The impedance tensor element $|Z_{xy}|$ for Yelta, and its error. The solid squares represent the absolute value of the impedance tensor, and the hollow squares mark the errors. The units of the impedance tensor are mv/km/gamma.

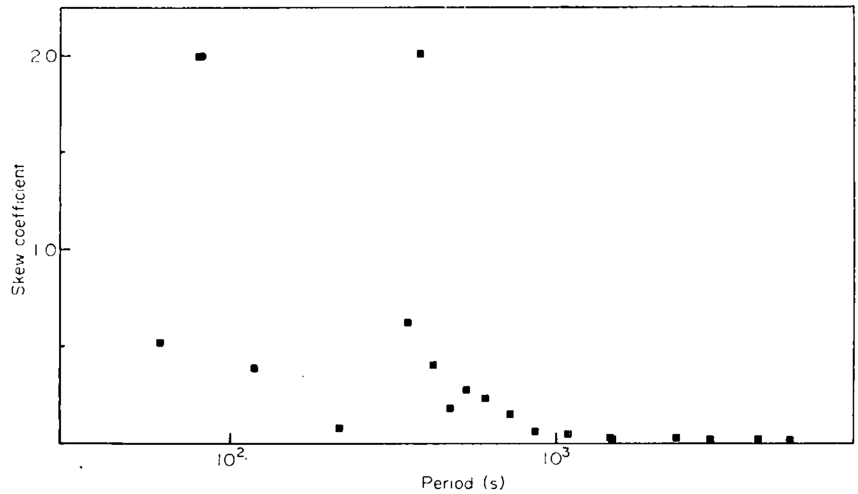

FIG. 4. Skew coefficient at Yelta as a function of period.

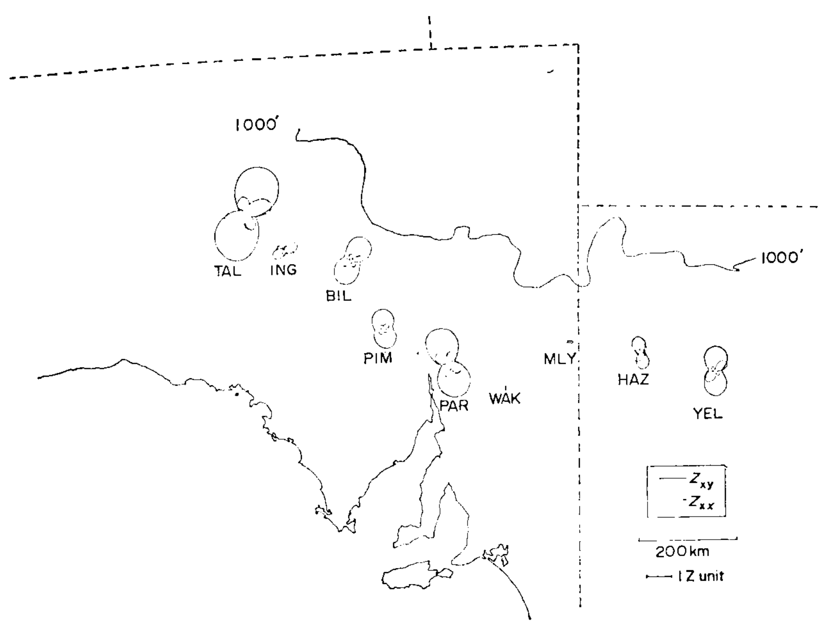

FIG. 5. Polar plots of the impedance tensors at a period 2270 s, with the 1000 ft depth contour of the Great Artesian Basin.

of 0·2 or less as for the long-period data at Yelta would generally be taken to indicate two-dimensional structure, (Swift 1967; Vozoff 1972). All the stations except Mulyungarie yielded similarly small skew values, indicating two-dimensionality.

In Fig. 5 the impedance tensors for the different stations are presented as polar plots, for a period of 2270 s. The radial distance and azimuth represent the absolute value of the tensor element and the rotation angle respectively, (see, for example, Berdichevskiy *et al.* 1970). The polar plots show a great variation in impedance magnitude across the traverse and two-dimensionality of structure is indicated by the pattern of four distinct lobes for Z_{xx}, together with the two-lobed pattern for Z_{xy}.

The determination of the principal axes of the impedance tensor should reveal directions parallel and perpendicular to the structural strike. It was decided to maximize the value of the off-diagonal term Z_{12} by rotating the measured Z_{ij}. The resulting principal axis orientation proved to be quite stable across the entire frequency spectrum and this result is given in Table 3 for each site.

Finally, apparent resistivities for the principal directions were calculated from the equation

$$\rho_{ij} = 0{\cdot}2\ T|Z_{ij}|^2$$

where ρ_{ij} is the apparent resistivity in ohm-m, T the period in seconds, and Z_{ij} is an off-diagonal element of the rotated impedance tensor. The apparent resistivities, together with their probable error bars, are shown in Fig. 6.

Interpretation

Several important facts are immediately evident from an inspection of the apparent resistivity curves (Fig. 6). Taking each station individually, in every case the ρ_{yx} curve is different from the ρ_{xy} curve, in many instances by an order of magnitude. The two-dimensionality of this effect has already been noted, though it will be shown later that this anisotropy is more local than regional, and is in fact a severe obstacle to the accurate interpretation of the data.

The dominant result of the experiment, however, stands out clearly above anisotropy effects, and is expressed by the very low apparent resistivities recorded at Waukaringa and Mulyungarie. This is also indicated in Fig. 2 by the high attenuation of the natural telluric signals at these sites relative to the stations on either side. The presence of a region of very high electrical conductivity has evidently been detected.

To commence the interpretation, an assumption was made that the electrical conductivity structure beneath Waukaringa and Mulyungarie is two-dimensional, so that a line from Pimba to Yelta direct would be at right angles to the strike. This assumption is supported by the tectonic lineations of the Adelaide geosyncline, and also quite independently by the magnetometer array data of Gough *et al.* (1972). Computations of particular two-dimensional models were then carried out, following the methods of Jones & Price (1970) and, in particular, using the programs of Jones & Pascoe (1971) and Pascoe & Jones (1972). Some 20 models were investigated, each one at several different frequencies. On the basis of certain initial assumptions, the final model was determined to within quite useful limits. An initial assumption was that an overburden of resistivity 10 ohm-m, 5 km deep, overlaid the whole region.

Table 3

Site:	TAL	ING	BIL	PIM	PAR	WAK	MLY	HAZ	YEL
Orientation:	30°	−10°	20°	0°	−20°	u.r.	u.r.	−10°	0°

Orientation of the principal axes of the impedance tensors (clockwise from north). ‘Unrotated’ is denoted by u.r.

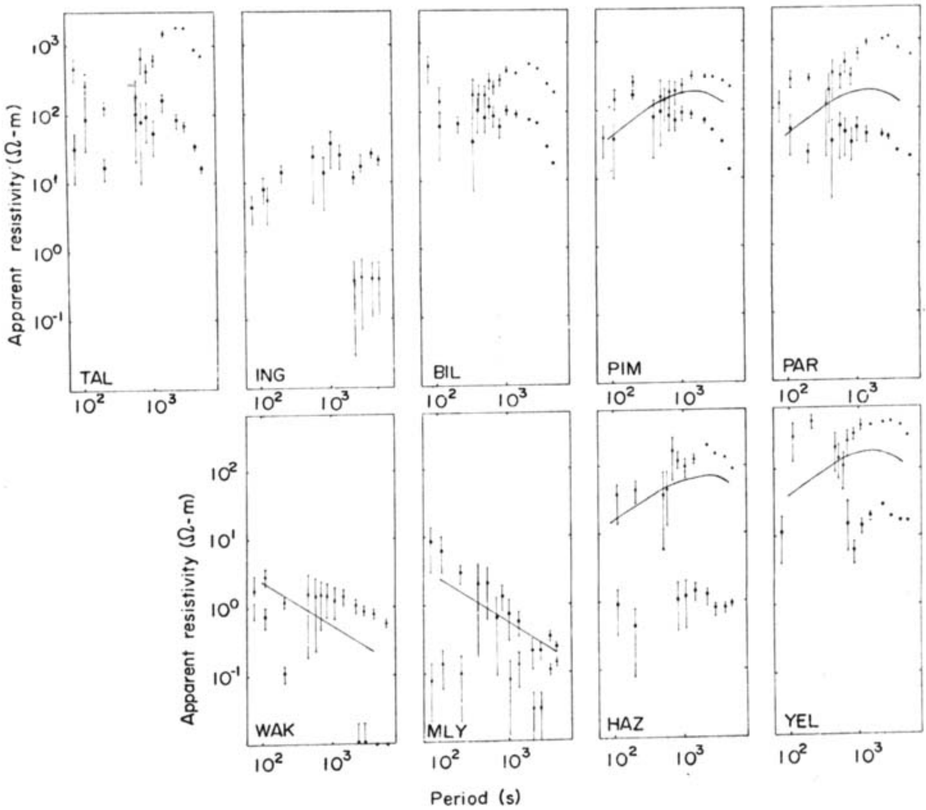

FIG. 6. Apparent resistivities calculated from impedance tensors which have been rotated into principal axes. The superimposed solid curves represent the theoretical ρ_{xy} curve for the model of ' best fit '. Solid squares represent ρ_{yx}, open triangles ρ_{xy}.

The resistivity of this overburden was taken from the values of the apparent resistivity at the lowest periods of Fig. 6, and is reasonable for the surface of inland Australia, which in places is covered with salt lakes, and is generally quite conductive. The depth of 5 km was taken from an estimate of the depth of sediment cover in the Adelaide Geosyncline (Stewart & Mount 1972); it may well be an overestimate for the overburden away from the synclinal area, but this is not likely to seriously affect the general features of the model.

The good conductor, modelled to lie between Waukaringa and Mulyungarie as shown schematically in Fig. 7, must have a resistivity as low as 0·1 ohm-m, and for this resistivity it must have a minimum thickness of 10 km; its maximum possible thickness is undetermined. The present data allow the uppermost surface of the good conductor to be arbitrarily near the surface of the ground; on the other hand it cannot be deeper than 10 km. The width of this feature is uncertain, but it must extend past Mulyungarie to the east and Waukaringa to the west. Modelling the good conductor against background resistivities of 100 ohm-m and 1000 ohm-m shows that the latter model (see Fig. 7) provides a slightly better fit. Theoretical apparent resistivity curves for this model are shown superimposed on the data of Fig. 6. The theoretical ρ_{xy} and ρ_{yx} curves are almost identical and only the former is illustrated. The smoothing effect of the uniform overburden no doubt plays a major role in this effect. This is an important result, for if the theoretical ρ_{xy} and ρ_{yx} curves are almost identical then the observed anisotropy is not caused by the two-dimensionality of this model, and remains

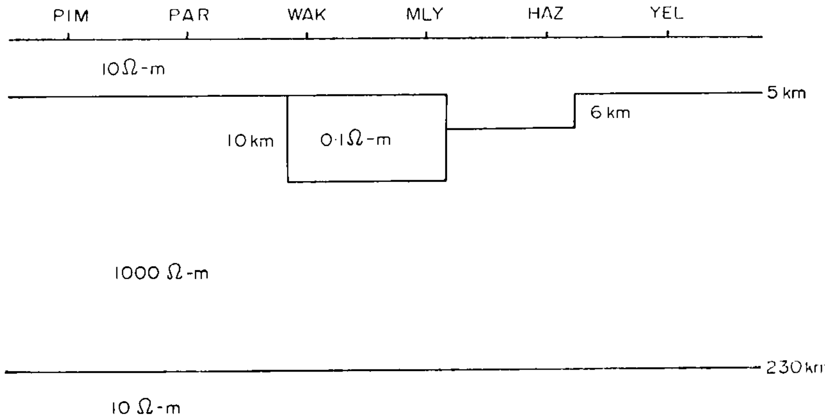

Fig. 7. A cross-section of the model (not to scale) which best fits the data.

to be explained. At this stage, the interpretation could proceed by assuming a layered earth under each station and then fitting model curves (e.g. Srivastava 1967) separately to each site.

Another feature of the apparent resistivity curves is their 'turn over' at long periods. If this is interpreted in terms of a highly conducting, lower region of resistivity 10 ohm-m, then the depth at which this region is encountered must be between 200 and 260 km.

Some discussion may now be given regarding the anisotropy, mentioned above for the data in hand, and in fact found almost universally in magnetotelluric experiments.

Because the principal axes of the impedance tensors at the different sites all showed an approximate north–south trend (Fig. 5), the anisotropy was originally thought to be the effect of a large, near-surface conductor to the north of the traverse (perhaps the Great Artesian Basin), superimposed upon the effect of the main model already described. The 1000 ft depth contour of the Great Artesian Basin is marked on Fig. 5, and it can be seen to be generally orthogonal to the principal axes of the impedance tensors. Fig. 8 shows the model examined to test this possibility: a sharp change occurring in the resistivity of surface sediments at a vertical contact. Also shown in Fig. 8 is the anisotropy which results, plotted as distance from the contact on the more resistive side. It can be seen that only within 25 km of the contact do the maximum and minimum apparent resistivity curves separate by an order of magnitude. This appears to render untenable the hypothesis that the observed anisotropy is caused by the Great Artesian Basin: for most observing sites are much further than 25 km away (see Fig. 5). It thus appears that the observed M–T anisotropy cannot reasonably be explained by induction on a regional scale; a likely alternative is, therefore, that it is caused by local channelling of telluric currents which are induced elsewhere, as in the cases studied by Dyck & Garland (1969), and Lilley & Tammemagi (1972). If this is so, then in the present case the current channelling mechanism has been particularly deceptive, because the resulting skew coefficients and rotation angles are indistinguishable from those caused by induction in a two-dimensional structure. The common occurrence of such anisotropy remains one of the greatest disadvantages of the magnetotelluric method.

Discussion

The major feature of the model is the large conductive block below Mulyungarie and Waukaringa. Perhaps surprisingly this is located just to the east of the Flinders Ranges and not under them. It is of great interest to compare this result with the

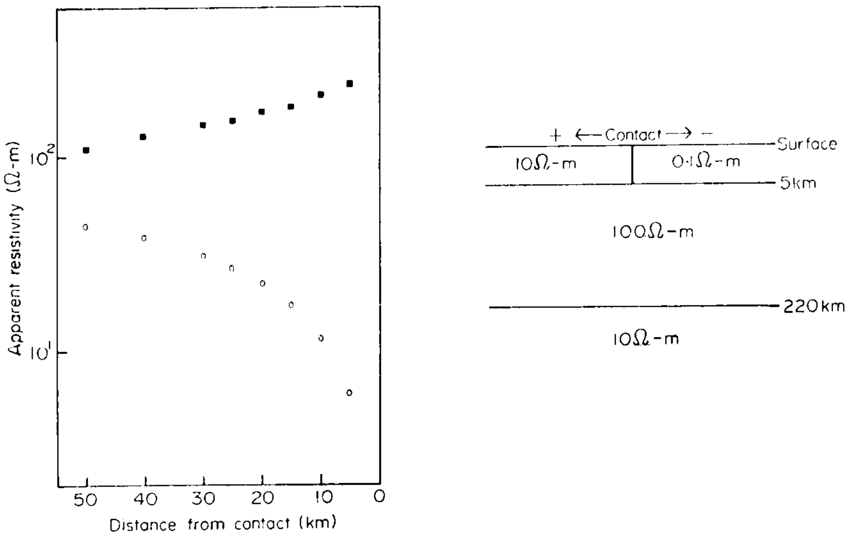

FIG. 8. Anisotropy as a function of distance, as modelled for the contact with the sediments of the Great Artesian Basin. The graph is drawn at a period of 2000 s for the positive side of the contact.

interpretation of the magnetometer array data, and model studies have been commenced for this specific purpose (Lilley & Tammemagi 1973); the preliminary results substantiate the presence and location of this conductive feature. The discovery of such a large volume of highly conducting rock in the crust is quite remarkable. As a case history it may be compared to the magnetotelluric work of Vozoff & Swift (1968), which described sediments of high conductivity in the North German basin: other major crustal conductors are mentioned by Garland (1971).

A tentative geological interpretation of this result is now presented. Dewey & Bird (1970) explain the formation of geosynclines in terms of miogeoclinal and eugeoclinal couplets, formed by the growth of continents by tectonic global processes. Oversby (1971) has concluded from geologic evidence that eastern Australia was formed by the interaction of the continental block with island arcs and trenches. Thus, the Adelaide Geosyncline would be the remnant of one couplet, and the other couplet would lie buried to the east, under Mulyungarie and Waukaringa. Whether the eastern material is itself more conductive or whether it is structurally weaker, resulting in greater fracture zones and higher porosity, and hence higher conductivity, is not known. There is the clear possibility that the sediments may contain a great deal of saline water.

It is also of interest to offer an interpretation for the deep zones of high conductivity commencing at a depth of about 250 km. The upper mantle is thought to be composed of peridotite (Ringwood 1969), the most conductive constituent of which is olivine, and the exponential decrease of olivine resistivity with temperature could provide an explanation. Combining the temperature-depth profile of MacDonald (1965) with the compilation of experimental conductivity-temperature results for 10 per cent fayalite olivine, (Duba & Lilley 1972), it is seen that by a depth of order 150 km and deeper the resistivity of olivine might be expected to decrease to about 10 ohm-m. *The proposed model is in reasonable agreement with this result.*

The general conductivity section, then, appears consistent with that found in a number of other continental magnetotelluric soundings (Keller 1971). The conductivity near the surface is high. As depth and pressure increase the rocks become more resistive, perhaps due to the reduction of their porosity; ultimately the rocks become more conductive again, perhaps due to the increasing effectiveness of the temperature-dependent semi-conduction mechanisms of olivine.

Acknowledgments

Above all else we are indebted to Professor D. I. Gough, who was leader of the project which supplied the magnetometer data, and who provided us with much stimulating discussion and instruction. We are grateful to the many people who assisted us in the field, and particularly we thank the station owners and managers at our sites; we much appreciated the generous hospitality of the Australian outback. The co-operation of the Land Research Unit of the C.S.I.R.O. and the use of their digitizer is appreciated. The authors enjoyed fruitful discussions with Professor E. J. Hannan, Dr J. R. Cleary, Dr A. R. Crawford, Dr A. G. Duba and Mr D. J. Bennett. One of us (H.Y.T.) was supported by an A.N.U. Research Scholarship.

Department of Geophysics and Geochemistry
Australian National University
Canberra

References

Berdichevskiy, M. N., Dubrovskiy, K. I., Sokolov, V. V. & Faynberg, E. B., 1970. Geoelectric characteristics of the earth's crust and upper mantle in Turkmenia, *Izv. Earth Phys*, **11**, 86–91.

Bevington, P. R., 1969. *Data reduction and error analysis for the physical sciences*, McGraw–Hill.

Cagniard, L., 1953. Basic theory of the magnetotelluric method of geophysical prospecting, *Geophysics*, **18**, 605–635.

Cantwell, T., 1960. *Detection and analysis of low frequency magnetotelluric signals*, Ph.D. thesis, Dept. of Geology and Geophysics, Massachusetts Institute of Technology.

Cleary, J. R. & Simpson, D. W., 1971. Seismotectonics of the Australian continent, *Nature*, **230**, 239–241.

Cleary, J. R., Simpson, D. W. & Muirhead, K. J., 1972. Variations in Australian upper mantle structure from observations of the Cannikin explosion, *Nature*, **236**, 111–112.

Dewey, J. F. & Bird, J. M., 1970. Mountain belts and the new global tectonics, *J. geophys. Res.*, **75**, 2625–2647.

Doyle, H. A., Everingham, I. B. & Sutton, D. J., 1968. Seismicity of the Australian continent, *J. geol. Soc. Aust.*, **15**, 295–312.

Duba, A. & Lilley, F. E. M., 1972. Effect of an ocean ridge model on geomagnetic variations, *J. geophys. Res.*, **77**, in press.

Dyck, A. V. & Garland, G. D., 1969. A conductivity model for certain features of the Alert anomaly in geomagnetic variations, *Can. J. earth Sci.*, **6**, 513–516.

Fournier, H., 1962. *Rev. Assoc. Ing. Gand* (*Mons*), **10**, 9–16.

Garland, G. D., 1971. Electrical conductivity anomalies—mantle or crust? *Comments on Earth Sciences: Geophysics*, **1**, 167–172.

Gough, D. I., Lilley, F. E. M. & McElhinny, M. W., 1972. A polarization-sensitive magnetic variation anomaly in South Australia, *Nature Phys. Sci.*, **239**, 88–91.

Gough, D. I., McElhinny, M. W. & Lilley, F. E. M., 1973. In preparation.

Gough, D. I. & Reitzel, J. S., 1967. A portable three-component magnetic variometer, *J. Geomagn. Geoelect.*, **19**, 203–215.

Jaeger, J. C., 1970. Heat flow and radioactivity in Australia, *Earth Planet. Sci. Letts*, **8**, 285–292.

Jones, F. W. & Price, A. T., 1970. The perturbations of alternating geomagnetic fields by conductivity anomalies, *Geophys. J. R. astr. Soc.*, **20**, 317–334.

Jones, F. W. & Pascoe, L. J., 1971. A general computer program to determine the perturbation of alternating electric currents in a two-dimensional model of a region of uniform conductivity with an embedded inhomogeneity, *Geophys. J. R. astr. Soc.*, **24**, 3–30.

Keller, G. V., 1971. Natural-field and controlled-source methods in electromagnetic exploration, *Geoexploration*, **9**, 99–147.

Lilley, F. E. M. & Tammemagi, H. Y., 1972. Telluric potentials recorded simultaneously at three sites near Canberra, A.C.T. (Australia), *Geoexploration*, **10**, 115–120.

Lilley, F. E. M. & Tammemagi, H. Y., 1973. Magnetotelluric and geomagnetic depth sounding methods compared in southern Australia, *Nature*, in press.

MacDonald, G. J. F., 1965. Geophysical deductions from observations of heat flow, *Geophysical Monograph* 8, ed. W. H. K. Lee, American Geophysical Union.

Oversby, B., 1971. Palaeozoic plate tectonics in the southern Tasman Geosyncline, *Nature Phys. Sci.*, **234**, 45–47.

Pascoe, L. J. & Jones, F. W., 1972. Boundary conditions and calculation of surface values for the general two-dimensional electromagnetic induction problem, *Geophys. J. R. astr. Soc.*, **27**, 179–193.

Ringwood, A. E., 1969. Composition and evolution of the upper mantle, *Geophysical Monograph* 13, ed. P. J. Hart, 1–17, American Geophysical Union.

Srivastava, S. P., 1967. Magnetotelluric two- and three-layer master curves, *Publ. Dom. Obs., Ottawa*, **35**, No. 7.

Stewart, I. C. F. & Mount, T. J., 1972. Earthquake mechanisms in South Australia in relation to plate tectonics, *J. geol. Soc. Aust.*, **19**, 41–52.

Swift, C. M., 1967. *A magnetotelluric investigation of an electrical conductivity anomaly in the south-western United States*, Ph.D. thesis, Dept. of Geology and Geophysics, Massachusetts Institute of Technology.

Vozoff, K., 1972. The magnetotelluric method in the exploration of sedimentary basins, *Geophysics*, **37**, 98–141.

Vozoff, K. & Swift, C. M., 1968. Magneto-telluric measurements in the North German Basin, *Geophys. Prospect.*, **16**, 454–473.

Whittaker, E. T. & Robinson, G., 1946. *The calculus of observations*, Blackie, London.